Journal of Biomechanics 93 (2019) 220–225

Contents lists available at ScienceDirect

Journal of Biomechanics

journal homepage: www.elsevier.com/locate/jbiomech
www.JBiomech.com

Short communication

Experimental analysis of the lower cervical spine in flexion with a focus on facet tracking

C. Muth-seng [a,*], D. Brauge [a,b,c], N. Soriau [a], B. Sandoz [a], M. Van den Abbeele [a], W. Skalli [a], S. Laporte [a]

[a] Institut de Biomécanique Humaine Georges Charpak, Arts et Métiers Paristech, 151 Boulevard de l'Hôpital, 75013 Paris, France
[b] Pôle Neuroscience-Neurochirurgie, Hôpital de Purpan, 31300 Toulouse, France
[c] Université Paul Sabatier, 31330 Toulouse, France

ARTICLE INFO

Article history:
Accepted 25 June 2019

Keywords:
Cervical spine
Functional spinal units
Flexion
Articular facets

ABSTRACT

Cervical traumas are among the most common events leading to serious spinal cord injuries. While models are often used to better understand injury mechanisms, experimental data for their validation remain sparse, particularly regarding articular facets. The aim of this study was to assess the behavior of cervical FSUs under quasi-static flexion with a specific focus on facet tracking. 9 cadaveric cervical FSUs were imaged and loaded under a 10 Nm flexion moment, exerted incrementally, while biplanar X-rays were acquired at each load increment. The relative vertebral and facet rotations and displacements were assessed using radio-opaque markers implanted in each vertebra and CT-based reconstructions registered on the radiographs. The only failures obtained were due to specimen preparation, indicating a failure moment of cervical FSUs greater than 10 Nm in quasistatic flexion. Facet motions displayed a consistent anterior sliding and a variable pattern regarding their normal displacement. The present study offers insight on the behavior of cervical FSUs under quasi-static flexion beyond physiological thresholds with accurate facet tracking. The data provided should prove useful to further understand injury mechanisms and validate models.

© 2019 Elsevier Ltd. All rights reserved.

1. Introduction

Over 250,000 spinal cord injuries are reported every year in the world, entailing high societal and personal costs (World Health Organisation report, 2013). Most are due to traumatic events and those occurring in the cervical region can lead to tetraplegia (NSCI, 2018). As such, a better understanding of the injury mechanisms of the cervical spine is key to help the development of tools for prevention, such as protective devices and relevant models.

While the biomechanics of the cervical spine under physiological loading have been widely studied *in vitro* (Panjabi et al., 1986, 2001; Moroney et al., 1988; Shea et al., 1991), there are far fewer studies regarding injury risks and mechanisms. *In vitro*, the mechanical properties and thresholds of the cervical in flexion have been studied on cervical Functional Spinal Units (FSUs) dynamically at high loading rates of 90 Nm/s (Nightingale et al., 2002, 2007), as well as on segments of 3 vertebrae quasi-statically at low loading rates of 5°/s (Shea et al., 1991), providing data on their mechanical behavior and strength. To the authors' knowledge, the failure thresholds in flexion and the mechanical response beyond 3.5 Nm of cervical FSUs at quasi-static rates remain unknown.

Cervical facet dislocations (CFD) are among the most commonly reported injuries. While the kinematics of CFD during high-speed loading were reported by Panjabi et al. (2007) using FSUs with muscle force simulation, identifying the influence of various parameters on the resulting behavior remains challenging. As such, it appears important to analyze lone FSUs without dynamic or muscular effects in order to assess the structural influence on facet kinematics. Furthermore, as dislocations are often associated with facet fractures (Foster et al., 2012), Quarrington et al. (2018, 2019) studied facet deflections and strains under low speed loading.

Recent advances have allowed fast and accurate 3D reconstructions of the human spine from medical images, either using biplanar X-rays (Humbert et al., 2009) or CT-scans, as well as for step-by-step motion tracking during *in vitro* testing via combination with X-ray imaging (Prud'Homme, 2014), hence yielding the possibility for quantitative facet joint tracking. The aim of this work is thus to study cervical FSUs in quasi-static flexion with a specific focus on facet tracking.

* Corresponding author.
E-mail address: christophe.muth-seng@ensam.eu (C. Muth-seng).

https://doi.org/10.1016/j.jbiomech.2019.06.022
0021-9290/© 2019 Elsevier Ltd. All rights reserved.

2. Material and methods

2.1. Test apparatus

A 6 degree-of-freedom spine tester was used. Its lower part was fixed and contained a 6-axis load cell whereas its upper part comprised a motor, which was allowed to move freely, thus exerting a pure moment. The samples were mounted on both parts of the spine tester using custom-made supports. The spine tester was placed inside a calibrated biplanar X-ray system (EOS Imaging SA., Paris, France) for motion tracking.

2.2. Specimen preparation

Four entire spines from PMHS (56 ± 9 years old, 2 females) were imaged using CT (Resolution: 0.47 × 0.47 × 0.8 mm), fresh-frozen for storage, then thawed at room temperature the day before dissection. They were stripped of muscles, leaving the osseoligamentous elements, and split into FSUs (C3-C4, C5-C6, C7-T1). Three FSUs were deemed unsuitable post inspection due to excessive degeneration, leaving 9 FSUs which were frozen for storage until the day before testing. After a second 24 h thawing cycle, Ø1mm drillings were performed allowing 5 radio-opaque fiducial markers (Ø2mm steel beads) to be implanted in each vertebra: 2 on the vertebral body, 1 on each articular apophysis and 1 on the spinous process (Fig. S1).

2.3. Custom support design

Using MITK-GEM (German Cancer Research Center - Division of Medical Image Computing, Heidelberg, Germany), each vertebra was reconstructed from the CT-scans. These accurate models were used to design the inner geometry of the supports, with the addition of a clearance for the surrounding soft tissues. The supports were printed in PLA using a 3D printer (Makerbot Industries, Brooklyn, USA) and ensured fixation of the FSU in the spine tester with 2 stainless steel screws through the pedicles of the upper vertebra and 5 threaded pins (1 through the upper vertebral body, 2 through the lower vertebral body and 1 through each spinous process) (Fig. 1). The remaining excess clearances were filled with resin and plasticine between the vertebrae and supports.

2.4. Test protocol

Specimens underwent three preconditioning cycles of 2 Nm of flexion-extension. A pure flexion moment at 1°/s was then applied in 2° rotation increments. Biplanar radiographs were taken at each load step after 30 s of torque relaxation. The protocol was carried out until failure occurred or until the motor reached its maximum output, i.e. 10 Nm moment.

2.5. Data processing

2.5.1. Vertebra motion tracking

The CT-based reconstruction were registered upon the initial X-ray images. The markers were tracked on each radiograph and the rigid registration from their initial positions to all the subsequent ones were computed, yielding the positioning of the vertebrae at each load step (Fig. S2). A local anatomical frame was computed as described in Rousseau et al. (2007) for each vertebra on every X-ray (Fig. 2a). The rotations of the upper vertebra were computed as the Bryant angles between its initial and subsequent anatomical frame positions using a xy'z'' sequence. These computations were made in the anatomical frame relative to the lower vertebra in its initial position.

2.5.2. Facet motion tracking

For each articular facet reconstruction, 8 peripheral points and their center were used to compute their best fit plane normal vector. A local frame was associated to each facet, located in its barycenter, with the Z axis aligned with the facet normal and the X axis defined by the intersection of the facet plane with the vertebral sagittal plane, indicating the anteroposterior direction of the facet surface (Fig. 2b). These facet frames were used to compute the displacements and rotations of the facets of the upper

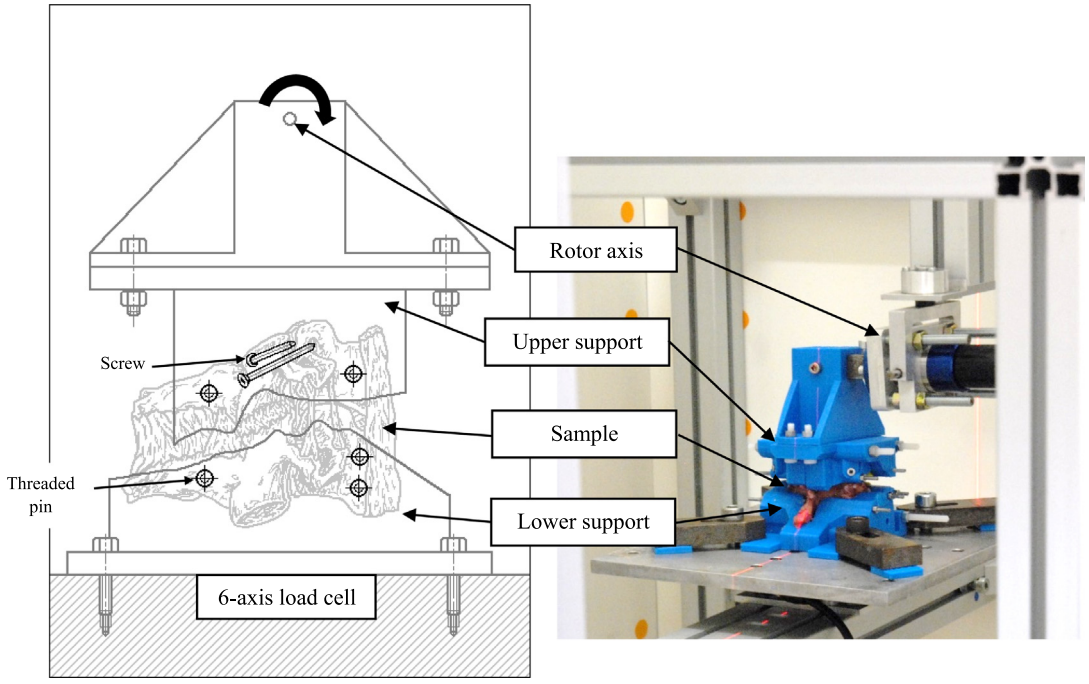

Fig. 1. Experimental set-up. The lower vertebra is fixed to the lower support via 3 threaded pins while the upper vertebra is fixated to the upper support with 2 pins and 2 screws. The lower and upper support are connected to a 6-axis load cell and a rotor axis respectively. The whole assembly is placed inside a biplanar X-ray EOS cabin.

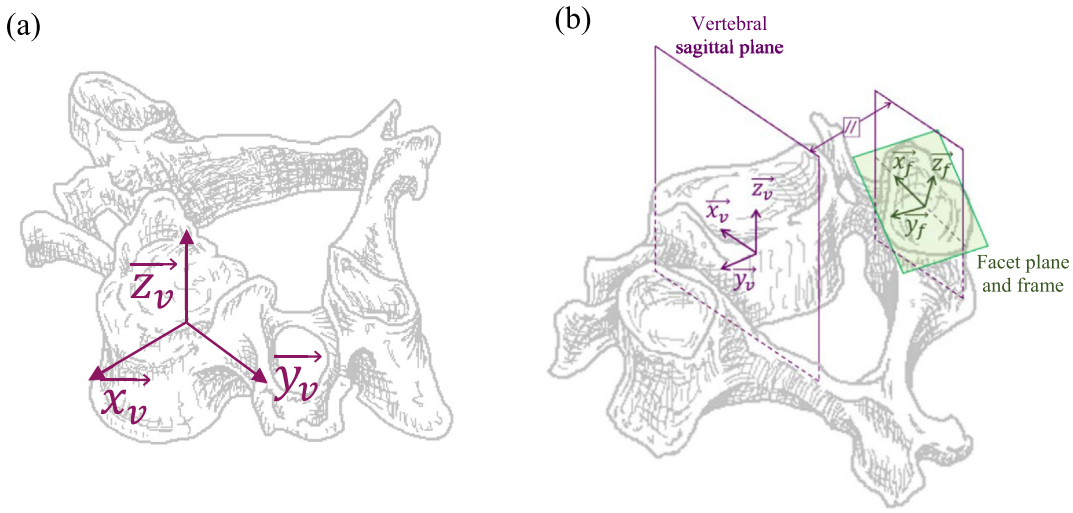

Fig. 2. (a) Anatomical frame associated to each vertebra computed for vertebral motion tracking similar to the description in Rousseau et al. (2007). (b) Facet frame with $\vec{z_f}$ normal vector of facet plane, $\vec{x_f}$ the intersection between the facet plane and the vertebral sagittal plane.

vertebra with respect to those of the lower vertebra. Additionally, displacements between the most anterior/posterior points of the upper and lower facet were computed.

2.5.3. Additional analysis

Reproducibility tests based on the Monte-Carlo method (S1) estimated 95% confidence intervals of 0.02° on vertebral rotation and up to 0.02 mm on facet displacements.

To assess posterior arch deformation, the vector going from the marker implanted on the spinous process to the mid-point between both articular apophysis was computed. The angle it made with the axial plane of the local vertebra frame was measured (Fig. S3) for each increment and the maximal deflection was assessed for each sample.

3. Results

Maximum posterior arch deflection was negligible (<5*10^{-4}°). Three failures were obtained, one due to rupture of the interspinous ligament at 6.62 Nm and the other two due to fracture of the posterior arch of the upper vertebra, close to the screw fixation, at 7.53 and 9.28 Nm. Inspection of the X-rays showed the ligament failure may have been due to damage during dissection prior to testing.

3.1. Vertebral mobility

The load-displacement curves for all FSUs are available in Fig. 3. For all specimens, a non-linear behavior was observed followed by

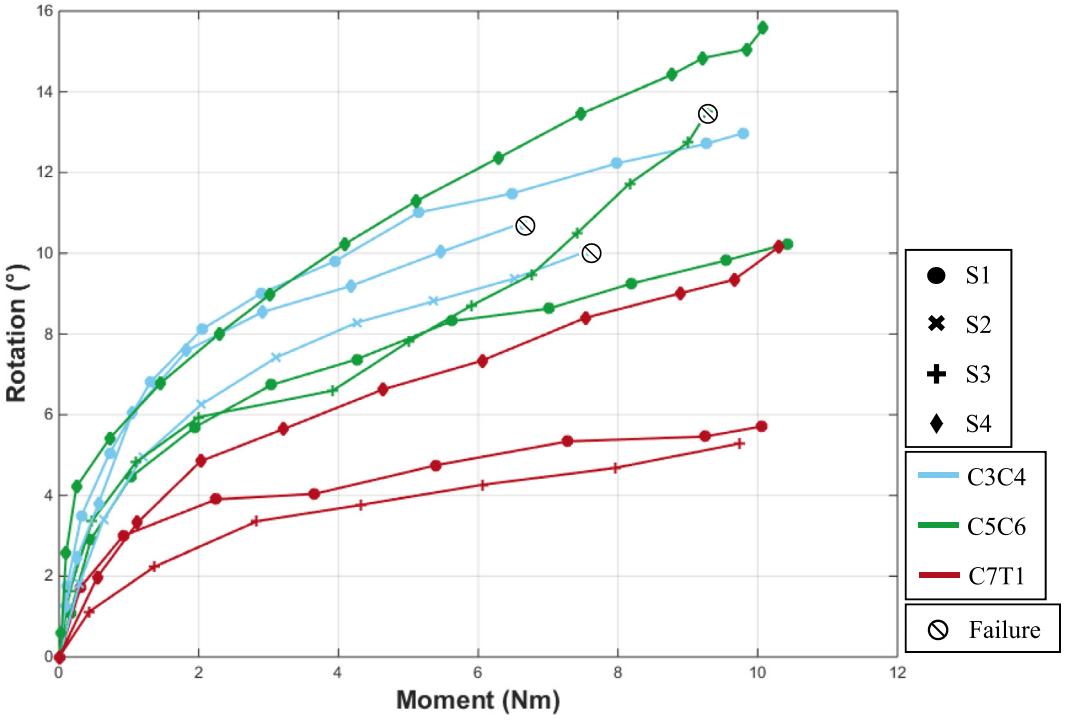

Fig. 3. Flexion angle between vertebral frames during hyperflexion test.

a quasi-linear response before reaching 3.5 Nm. At 6 Nm, no failure was observed and the flexion angle between vertebrae ranged from 4° to 11.8°. At 10 Nm, the flexion angle ranged from 5.3° to 15.3° for the 6 remaining FSUs (Table S1).

3.2. Facet motions

Facet sagittal rotations were consistent with vertebral sagittal rotations. Facet relative displacements (Fig. 4) exhibited a non-linear behavior followed by a linear response. The center of the facets of the upper vertebra steadily moved in the anterior direction of the facet frame. Their lateral displacements ranged from −1.03 to 0.16 mm in the non-linear portion and remained stable afterwards. Their normal displacements remained quasi-linear after 2 Nm. They ranged from −1.67 mm to 1.20 mm. Displacements between the anterior and posterior points ranged from −1.14 to 3.19 mm and −1.98 to 3.52 mm respectively.

4. Discussion

The aim of this present work was to study cervical FSUs in quasi-static flexion with accurate facet tracking. An original protocol was proposed combining CT and biplanar X-ray imaging, which ensured the accuracy of geometry modeling and motion tracking respectively.

The load-displacement behavior of 9 cervical FSUs was recorded under the application of a 10 Nm flexion moment, exerted incrementally, using biplanar X-rays, acquired at each load increment. The registration of the CT-based reconstructions and the tracking of markers on each pair of radiographs allowed tracking the relative motions between vertebrae and between facet surfaces.

4.1. Vertebral mobility

The non-linear load-displacement curve of the cervical spine due to the neutral zone and hyperelastic response of the ligamentous structures and disks has been widely reported in *in vitro* studies (Panjabi et al., 1986, 2001). Comparative flexion angle between the present work and the literature under various moment loads are given in Table 1. Flexion angles complied with the ranges observed by Panjabi et al. (2001) under a 1.0 Nm pure moment and Moroney et al. (1988) under a 1.8 Nm moment and 48 N compression, though they appeared lower than what Nightingale et al. (2002) observed under a 3.5 Nm pure moment. However, the latter released the load between load steps.

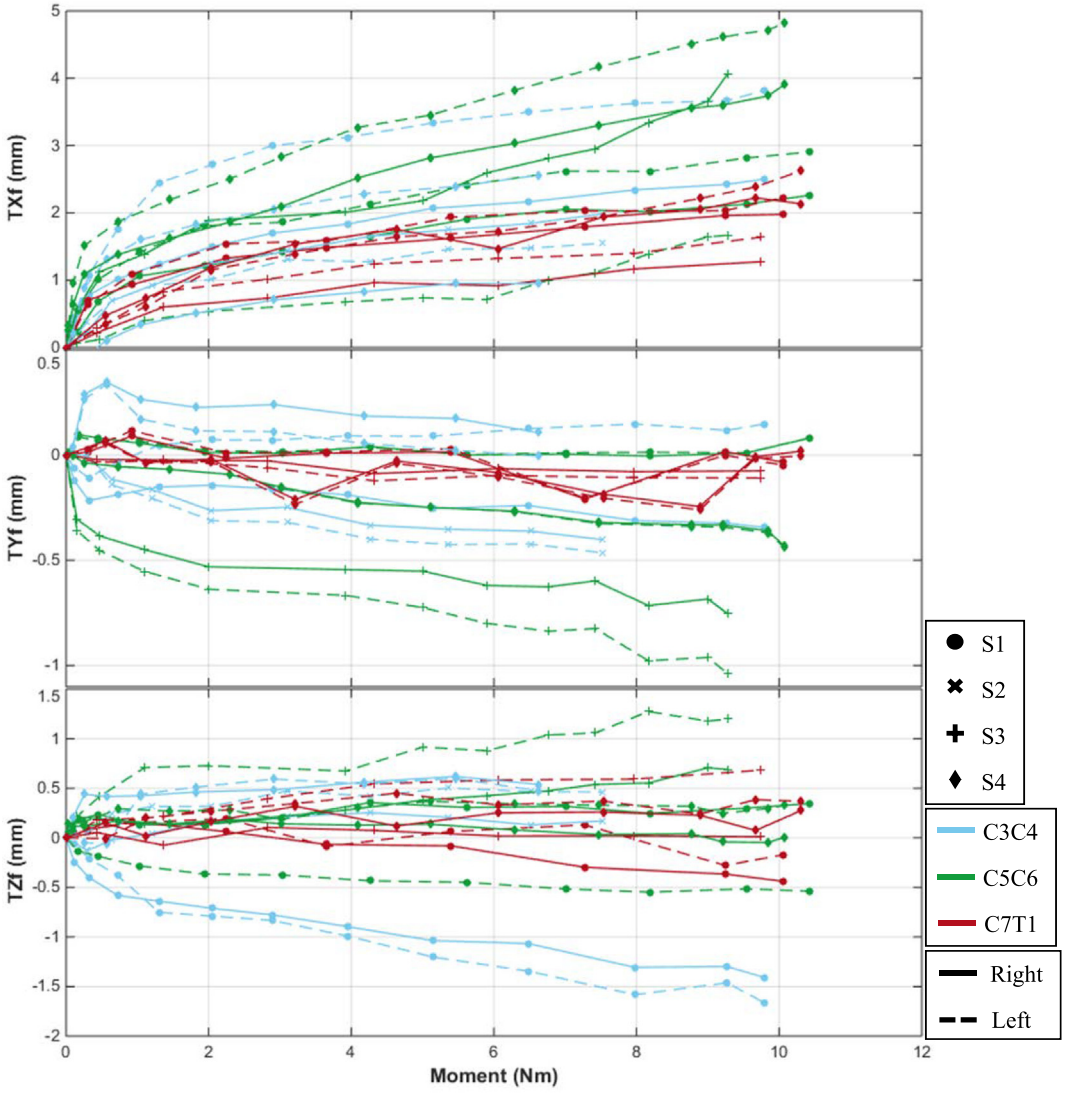

Fig. 4. Facet displacements. (a) Antero-posterior displacements, along $\vec{x_f}$ (b) Normal displacements, along $\vec{z_f}$ (c) Lateral displacements, along $\vec{y_f}$.

Table 1
Comparative range of motion from *in vitro* flexion studies at 1.0, 1.8 and 3.5 Nm from literature.

Moment (Nm)	Study	Flexion angle (°)		
		C3-C4	C5-C6	C7-T1
1.0	Panjabi et al. (2001)	4.3 ± 2.9	5.5 ± 2.6	
	Present study	4.32–4.93	3.69–6.10	1.68–2.65
1.8	Moroney et al. (1988)	5.55 ± 1.84	5.55 ± 1.84	5.55 ± 1.84
	Present study	5.71–6.82	5.08–7.40	2.80–4.09
3.5	Nightingale et al. (2002)	12.2 ± 1.45	13.6 ± 2.71	7.22 ± 3.17
	Present study	7.80–9.40	7.05–9.60	3.56–6.13

4.2. Sample failure

Due to test bench limitations, samples could only be tested up to a flexion moment of 10 Nm. Three failures could be observed due to fixation or dissection. Hence the failure moment seems to be greater than 10 Nm in quasi-static flexion loading. This is consistent with the reported failure for dynamic pure moments of 17.4 ± 6.2 Nm for females (Nightingale et al., 2002) and 21.5 ± 6.8 Nm for males (Nightingale et al., 2007). Comparatively, reported failure for quasi-static pure moment application on segments of 3 vertebrae were 7.0 ± 3.2 Nm for C2-C5 and 12.1 ± 0.5 Nm for C5-T1 (Shea et al., 1991).

Due to technical issues, the samples underwent 2 freeze-thaw cycles, but this has a limited effect on the mechanical properties of ligaments (Amout et al., 2013; Huang et al., 2011) and intervertebral discs (Tan and Uppuganti, 2012).

4.3. Facet motions

Facet tracking has rarely been performed in the literature. While Panjabi et al. (2007) did report facet kinematics, the FSUs used in their study were loaded at high-speed with muscle force simulation and a compressive pre-load, making the comparison difficult.

Overall, facet motions exhibited a non-linear portion followed by a more linear behavior. Facets of the upper vertebra persistently moved in the anterior direction of the facet, which is consistent with the relative facet sliding expected during flexion under pure moments. Displacements normal to the facet surfaces exhibited a linear response post neutral zone with no observable pattern, suggesting that facets moved closer, away or remain at a steady distance throughout flexion. Facet lateral displacements appeared to remain constant following the non-linear portion, indicating a small lateral shift and possible instability in the neutral zone, which the free-moving motor did not counteract.

Facet sagittal rotations were consistent with the measured vertebral rotations, which was expected as computations consider vertebrae as rigid bodies. While the low posterior arch deflection appears to confirm this assumption, it contrasts with Quarrington et al. (2019) reporting facet sagittal deflections of 0.25 ± 0.18° under 10° flexion with 50 N compression. However, on the one hand, they used marker carriers which could have amplified deflection measurements, and on the other hand this study used pins going through the spinous processes, which may have rigidified the vertebrae, explaining the low posterior arch deflection. Methodology regarding facet tracking and fixations needs to be further explored in future studies.

The results obtained, namely the vertebral motions beyond 3.5 Nm, as well as the facet displacements, should prove useful for model validation. Further studies could use this protocol while applying a higher load so as to analyze injury mechanisms. Moreover, the approach used in this study combining *in vitro* testing with imaging techniques to model and track particular areas of interest could be used to further study the human spine and other anatomical structure.

Declaration of Competing Interest

None declared.

Acknowledgements

The authors wish to express their gratitude to the Fédération Française de Rugby and the ParisTech-BiomecAM chair program, financed by Société Générale, Covea, Proteor and Fondation Cotrel, for their support. They would also like to thank Sylvain Persohn for his technical expertise and precious help in designing and carrying out the experiments.

Appendix A. Supplementary material

Supplementary data to this article can be found online at https://doi.org/10.1016/j.jbiomech.2019.06.022.

References

Amout, N., Myncke, J., Vanlauwe, J., Labey, L., Lismont, D., Bellemans, J., 2013. The influence of freezing on the tensile strength of tendon grafts: a biomechanical study. Acta Orthop. Belg. 79, 435–443.

Foster, B.J., Kerrigan, J.R., Nightingale, R.W., Funk, J.R., Cormier, J.M., Bose, D., Sochor, M.R., Ridella, S.A., Ash, J.H., Crandall, J., 2012. Analysis of cervical spine injuries and mechanisms for CIREN rollover crashes. In: International IRCOBI Conference on the Biomechanics of Injury, Dublin, Ireland.

Humbert, L., De Guise, J.A., Aubert, B., Godbout, B., Skalli, W., 2009. 3D reconstruction of the spine from X-rays using parametric models based on transversal and longitudinal inferences. Med. Eng. Phys. 3 (6), 681–687.

Huang, H., Zhang, J., Sun, K., Zhang, X., Tian, S., 2011. Effects of repetitive multiple freeze-thaw cycles on the biomechanical properties of human flexor digitorum superficialis and flexor pollicis longue tendons. Clin. Biomech. 26, 419–423.

Moroney, S.P., Schultz, A.B., Miller, J.A.A., Andersson, G.B.J., 1988. Load-displacement properties of lower cervical spine motion segments. J. Biomech. 21, 769–779.

National Spinal Cord Injury Statistical Center, 2018. Spinal Cord Injury Facts and Figures at a Glance.

Nightingale, R.W., Winkelstein, B.A., Knaub, K.E., Richardson, W.J., Luck, J.F., Myers, B.S., 2002. Comparative strengths and structural properties of the upper and lower cervical spine in flexion and extension. J. Biomech. 35, 725–732.

Nightingale, R.W., Chancey, V.C., Ottaviano, D., Luck, J.F., Tran, L., Prange, M., Myers, B.S., 2007. Flexion and extension structural properties and strengths for male cervical spine segments. J. Biomech. 40, 535–554.

Panjabi, M.M., Summers, D.J., Pelker, R.R., Videman, T., Friedlaender, G.E., Southwick, W.O., 1986. Three-dimensional load-displacement curves due to forces on the cervical spine. J. Orthop. Res. 4, 152–161.

Panjabi, M.M., Crisco, J.J., Vasavada, A., Oda, T., Cholewicki, J., Nibu, K., Shin, E., 2001. Mechanical properties of the human cervical spine as shown by three-dimensional load-displacement curves. Spine 26 (24), 2692–2700.

Panjabi, M.M., Simpson, A.K., Ivancic, P.C., Pearson, A.M., Tominaga, Y., Yue, J.J., 2007. Cervical facet joint kinematics during bilateral facet dislocation. Eur. Spine J. 16, 1680–1688.

Prud'Homme, M., 2014. Evaluation Clinique et biomécanique d'un implant de stabilisation dynamique du rachis lombaire. PhD. thesis. Arts et Métiers Paristech, Paris.

Quarrington, R.D., Costi, J.J., Freeman, B.J.C., Jones, C.F., 2018. Quantitative evaluation of facet deflection, stiffness strain and failure load during simulated cervical spine trauma. J. Biomech. 72, 116–124.

Quarrington, R.D., Costi, J.J., Freeman, B.J.C., Jones, C.F., 2019. The effect of axial compression and distraction on cervical facet mechanics during anterior shear, flexion, axial rotation, and lateral bending motions. J. Biomech. 83, 205–213.
Rousseau, M.-A., Laporte, S., Chavary-Bernier, E., Lazennec, J.-Y., Skalli, W., 2007. Reproducibility of measuring the shape and three-dimensional position of cervical vertebrae in upright position using the EOS stereoradiography system. Spine 32 (23), 2569–2572.
Shea, A., Edwards, W.T., White, A.A., Hayes, W.C., 1991. Variations of stiffness and strength along the human cervical spine. J. Biomech. 24 (2), 95–107.
Tan, J.S., Uppuganti, S., 2012. Cumulative multiple freeze-thaw cycles and testing does not affect subsequent within-day variation in intervertebral flexibility of human cadaveric lumbosacral spine. Spine 37 (20), E1238–E1242.
World Health Organisation, International Spinal Cord Society, 2013. International Perspectives on Spinal Cord Injury.